

# CONCEPTUAL DESIGN OF THE BETA = 0.86 CAVITIES FOR THE SUPERCONDUCTING LINAC OF ESS

G. Devanz, J. Plouin, CEA-Saclay, 91191 Gif-sur-Yvette, France

## Abstract

CEA-Saclay is in charge of the design, the fabrication and the tests of the superconducting high beta cavities for the high energy part of the European Spallation Source (ESS) linac. This paper reports the actual status of the RF and mechanical design of these cavities. According to ESS specifications, these cavities will be 5-cells elliptical, with frequency 704 MHz and  $\beta = 0.86$ . They will work in pulsed mode, with a beam current initially equal to 50 mA. The target accelerating gradient is 18 MV/m on the linac, and 20 MV/m in vertical tests. For the RF design, the cavity efficiency and the peak fields were optimized, while the feasibility of the external coupling with RF power was taken into account. Attention was also paid to the HOM frequencies and impedances and to their future extraction. Coupled RF/mechanical FEM calculations have been carried out and the Lorentz detuning, critical for a pulsed mode cavity, is lowered by the insertion of stiffening rings.

## INTRODUCTION

The superconducting part of the ESS proton linac consists in a 352.21 MHz spoke resonator section followed by two different sections of 704.42 MHz 5-cell elliptical bulk niobium cavities. The medium beta and the high beta cavities are grouped in cryomodules of 4 and 8 cavities respectively. The high beta section accelerates protons from 500 MeV up to the linac output energy of 2.5 GeV corresponding to a reduced velocity range  $\beta=v/c$  from 0.76 to 0.96. The specifications for the  $\beta = 0.86$  cavities are shown in table 1:

Table 1: Relevant specifications for the design of the high beta elliptical cavities

Frequency (MHz)	704.42
Number of cells	5
Operating temperature (K)	2
Maximum surface field in operation (MV/m)	40
Nominal Accelerating gradient (MV/m)	< 18
$Q_0$ at nominal gradient	> 6e9
Repetition rate (Hz)	14
Beam pulse length (ms)	2.86
Beam current (mA)	50
Nominal peak power transmitted by power couplers (kW)	< 900

The cavity design must take into account all the aspects related to high power pulsed beam operation, in particular the feasibility of RF coupling, the control of high order mode excitation, damping and propagation, and the mechanical stability of the cavity itself.

## RF DESIGN

One of the main parameters in the design of a multi-cell cavity is the cell-to-cell coupling  $\kappa$ . Choosing a low  $\kappa$  value emphasizes the cavity efficiency only. With increasing  $\kappa$ , the efficiency is reduced but major gains numerous: it is easier to achieve an even field distribution in the cavity, and therefore to control the homogeneity of the peak surface fields among the cells. The frequency separation between the accelerating mode and its neighbor is also increased. Even more important for a high current application the high  $\kappa$  translates into higher iris diameters, and better high order mode (HOM) propagation. We have investigated designs with different  $\kappa$  values from 1.1 to 2.5 for the  $\beta = 0.86$  cavity. The conclusion was that the loss in cavity efficiency was excessive above  $\kappa = 2$ .

One important geometrical parameter for designing a multi-cell elliptical cavity is the wall angle, related to mechanical stability, sensitivity to Lorentz force detuning (LFD) and the ease of cavity preparation (chemical etching, high pressure water rinsing and drying) which is a key point for achieving cavity performances. Based on experience with  $\beta = 0.5$  and  $\beta = 0.65$  with which we have explored wall angles between 5.5 and 8.5 degrees [1,2], we have chosen a minimum wall angle of 8 degrees. This of course restricts the range of geometrical cell parameters accessible for cavity optimization for peak fields in particular.

The main cavity parameters of the design are shown in table 2:

Table 2: High beta cavity RF properties

Geometrical beta	0.86
Iris diameter (mm)	120
Cell to cell coupling $\kappa$ (%)	1.8
$\pi$ and $4\pi/5$ mode separation (MHz)	1.2
Epk/Eacc	2.2
Bpk/Eacc (mT/(MV/m))	4.3
Maximum. $r/Q$ ( $\Omega$ )	477
Optimum beta	0.92
G ( $\Omega$ )	241

Taking into account the cryogenic duty cycle, the average power dissipated in one cavity at 18 MV/m is less than 5.3 W at the  $Q_0$  specification.

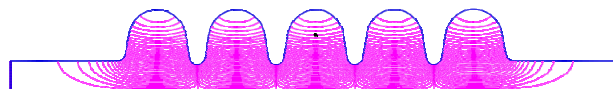


Figure 1:  $\beta = 0.86$  cavity geometry.

The fundamental mode is shown on figure 1 and the fundamental passband modes impedance is shown on figure 2. In the energy range of the high beta section (beta between 0.76 and 0.96) besides the accelerating mode, only the  $4\pi/5$  mode has significant impedance. However this cannot be avoided in this type of cavities.

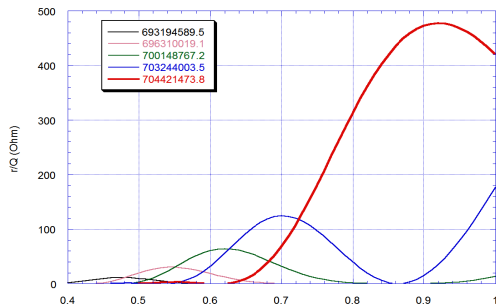


Figure 2: fundamental passband modes  $r/Q$  as a function of beta.

*External Coupling and End-groups*

The matched  $Q_{ext}$  at the specified beam current and nominal gradient is  $7.1 \cdot 10^5$ . The power coupler connection is a 100 mm,  $50 \Omega$  coaxial line. The beam tube diameter of 130 mm was chosen as a starting point for the design of the end-groups. However, taking into account the integration of the coupler port and helium vessel on the cavity sets constraints on the minimum distance between the power coupler and the closest cavity iris. This setup requires an antenna penetration which exceeds 12 mm in order to achieve the correct  $Q_{ext}$ . After enlarging the beam tube diameter to 140 mm the correct coupling is obtained for an antenna penetration of 9 mm (fig. 3) for a distance  $L_c$  (see fig. 4) between the coupler and iris of 30 mm. This calculation was done in the case of a flat antenna tip with a 5mm filet.

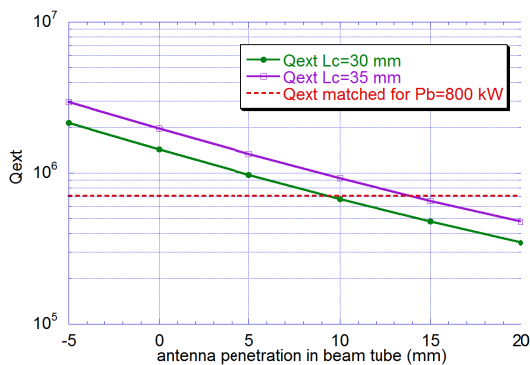


Figure 3:  $Q_{ext}$  as a function of antenna penetration.

An improvement of the coupling of the order of 15% is obtained by giving the antenna tip a conical shape as shown on figure 4, which permits a reduction of the penetration by 2 mm.

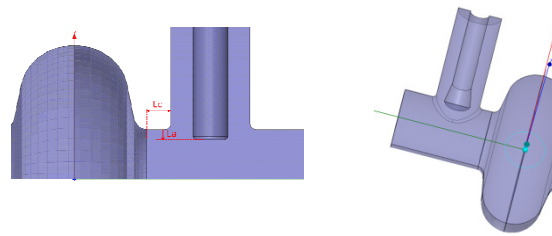


Figure 4: flat and conical antenna tip geometries.

One benefit of the beam tube enlargement is a reduction of the cutoff frequency for the HOMs.

**MONOPOLE HOMS**

Calculation of high order modes in the cavity has been carried out. Focus has been given to the study of the TM monopole modes since their excitation is more relevant than the excitation of dipole modes for the beam dynamics in a proton linac [3,4]. The Superfish (monopoles only), COMSOL and HFSS codes have been used and it has been checked that their result are consistent using the proper meshing quality.

Only two HOM monopole bands are below cutoff. During the cavity shape optimization the first monopolar band had to be shifted to prevent the two lowest frequency modes to sit close to the harmonic of the fundamental frequency ( $f_2 = 1408.8$  MHz). The first of these modes (see fig. 5) has been shifted 12 MHz above the  $f_2$  frequency to prevent its excitation.

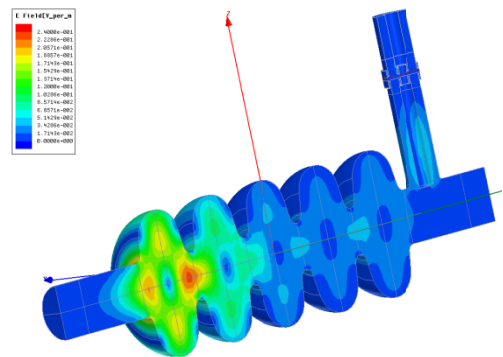


Figure 5: Lowest frequency TM monopole mode.

In order to assess the damping provided by the normal conducting parts of the power coupler and bellows located between the cavities, these elements have been included in the EM simulations. The result for the non propagating monopole TM modes is shown in table 3.

Table 3: Non-propagating TM monopoles

Frequency (MHz)	Max. r/Q (Ohm)	Q
First monopolar band		
1420.3	8	$1.58 \cdot 10^5$
1421.9	17	$4.30 \cdot 10^3$
1431.7	4	$3.22 \cdot 10^4$
1442.8	29	$3.30 \cdot 10^4$
1456.0	60	$4.41 \cdot 10^4$
Second monopolar band (TM02)		
1480.1	5	$1.98 \cdot 10^4$
1491.5	17	$1.3310^4$
1431.7	4	$1.40 \cdot 10^4$
1518.2	4	$1.8710^4$
1527.9	0.2	$4.5710^4$

The maximum value of the r/Q given in this table is for the beta range of 0.76 to 0.96. The RF window of the power coupler has been included in the simulation in order to take into account its transmission characteristics. This is an idealized case however since the boundary condition at the air side of the coupler is a matched port in our computation. In the actual setup a doorknob or a T-bar transition would ensure the connection between the coupler and the rectangular waveguide of the RF network, and present different transmission characteristics. The transmission of the window around the considered frequencies is enough to increase the damping by providing coupling to the air side as can be observed on the field distribution of the 1456 MHz mode on figure 6.

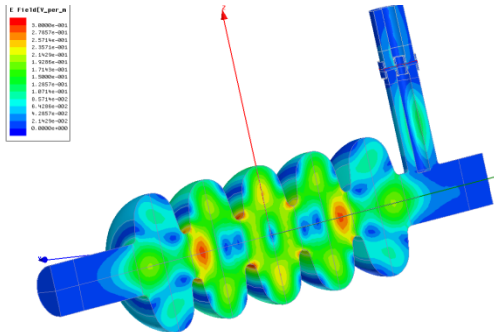


Figure 6: highest impedance monopole HOM below cutoff (1456 MHz).

Even if the quality factors of the monopole HOMs are promisingly low, HOM coupler will be designed to investigate if higher damping coefficient could be achieved. We already know that the damping of all dipole and quadrupole HOM polarizations cannot be effectively provided by the power coupler.

## MECHANICAL DESIGN

### Lorentz Detuning

Since these cavities are aimed to work in pulsed mode, it is important to minimize their sensitivity to Lorentz

detuning. To this intend stiffening rings are placed between the cavity cells. The static Lorentz coefficient,  $K_L = \Delta f / E_{acc}^2$ , measures the resonance frequency shift produced by the mechanical deformation induced by the electromagnetic field in continuous wave. The positions of the stiffening rings and the cavity thickness have been optimized in order to minimize  $|K_L|$  when the cavity has fixed extremities. The result is a cavity thickness of 3.6 mm and a stiffening rings radius of 84 mm. With these values,  $|K_L|$  is equal to  $0.36 \text{ Hz}/(\text{MV}/\text{m})^2$  for cavity with fixed ends. An exhaustive list of the corresponding RF/mechanical parameters is given in table 4.

Table 4: Mechanical characteristics of the cavity

$K_L$ fixed ends (Hz/(MV/m) <sup>2</sup> )	-0,36
$K_L$ free ends (Hz/(MV/m) <sup>2</sup> )	-8.9
Stiffness (kN/mm)	2.59
$\Delta f / \Delta z$ (kHz/mm)	197
max VM stress /1mm (MPa)	25
$K_P$ fixed ends (Hz/mbar)	4,85
$K_P$ free ends (Hz/mbar)	-150
max VM stress /1bar fixed (MPa)	12
max VM stress /1bar free (MPa)	15

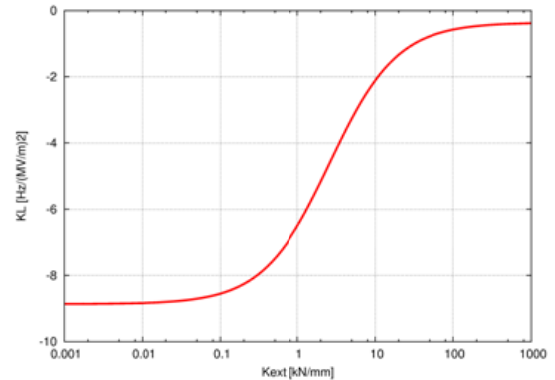


Figure 7: Static Lorentz detuning as a function of external stiffness.

The actual static Lorentz detuning depends upon the external stiffness  $K_{ext}$  experienced by the cavity during operation, which is given by the tuner and helium tank stiffness. Figure 7 shows the variation of  $K_L$  with respect to  $K_{ext}$  calculated by the analytic formula:

$$K_L = K_{L\infty} + \frac{\Delta f \vec{F}_{\infty} \cdot \vec{u}_z / E_{acc}^2}{\Delta z K_{ext} + K_{cav}}$$

From our experience with other cavities (HIPPI), we expect a value around 30 kN/mm for the overall external stiffness, which leads to  $|K_L|$  around  $1 \text{ Hz}/(\text{MV}/\text{m})^2$ . For the nominal accelerating gradient  $E_{acc} = 18 \text{ MV}/\text{m}$  the corresponding static detuning is 324 Hz (1/3 of the loaded cavity bandwidth).

### Tuning System

The dynamic Lorentz detuning in pulsed operation will be compensated by a fast tuning system. We should use a

Saclay V type piezo tuner, since this type of tuner has been successfully used for Lorentz detuning compensation in pulsed mode with the CARE/HIPPI cavity [5]. The tuner should be inserted between the cavity flange and the helium tank (fig. 8), likewise the SPL  $\beta=1$  cavity design [6].

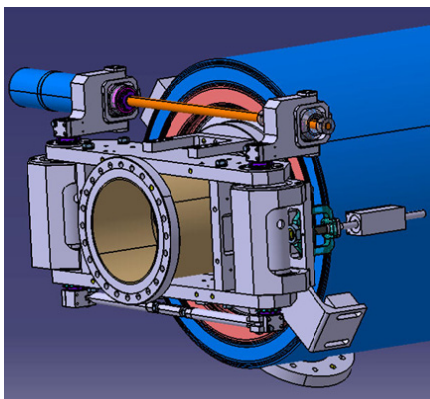


Figure 8: Tuner integration on the cavity with a Ti helium vessel.

### *Resistance to Differential Pressure*

$K_p$  measures the resonance frequency shift induced by the differential pressure  $P$  between outside and inside of the cavity:  $K_p = \Delta f/P$ . The coefficients given in table 4 correspond to elastic deformation.

Before operation the cavity should be subjected to safety pressure tests, and we investigated how it could be then plastically deformed. We calculated the plastic deformation involved when the fixed ends cavity experiences the following pressure cycle:  $0 \rightarrow 5 \text{ bars} \rightarrow 0$ . The maximal residual deformation is less than 7 microns and is situated in the outer cells (fig.9). The consecutive frequency detuning is 560 Hz.



Figure 9: Cavity residual deformation (amplified) after a 5 bar differential pressure cycle.

## REFERENCES

- [1] J. -L. Biarrotte et al., "704 MHz superconducting cavities for a high intensity proton accelerator", Proc. of SRF99, Santa-Fe, NM, 1999.
- [2] G. Devanz et al., "Stiffened medium beta 704 MHz elliptical cavity for a pulsed proton linac", Proc. of SRF07, Beijing, 2007.
- [3] M. Schuh et al. "Influence of higher order modes on the beam stability in the high power superconducting proton linac", Phys. Rev. ST Accel. Beams 14, 051001 (2011).
- [4] S. -H. Kim, "Higher Order Mode Analysis of the SNS Superconducting Linac", Proc. of PAC01, Chicago, IL, 2001.

- [5] G. Devanz et al. "High Power Pulsed Tests of a beta=0.5 5-cell 704 MHz Superconducting Cavity". SRF 2011, these proceedings.
- [6] J. Plouin et al. "Optimized RF design of 704 MHz beta=1 cavity for pulsed proton drivers". SRF 2011, these proceedings.